Hindawi
Journal of Advanced Transportation
Volume 2023, Article ID 2816407, 12 pages
https://doi.org/10.1155/2023/2816407

Research Article

A Coordinated Allocation Method for Right-Turn Strategy at Signalized Intersections with Optimal Pedestrian and Vehicle Delays

Yu Bai and Wanyan Luo

Key Laboratory of Road and Traffic Engineering of the Ministry of Education, Tongji University, Shanghai 200000, China

Correspondence should be addressed to Wanyan Luo; 2131287@tongji.edu.cn

Received 25 February 2023; Revised 15 October 2023; Accepted 26 October 2023; Published 10 November 2023

Academic Editor: Jinjun Tang

With strict enforcement of pedestrian right of way at all intersections, the inappropriate right-turn resource allocation from a spatial and temporal perspective will lead to a reduction in the operational efficiency of the intersection. In this paper, three spatiotemporal resource allocation schemes for right-turning vehicles are proposed, considering the vehicle and pedestrian traffic efficiency in all directions of the intersection. To minimize vehicle and pedestrian delay at the intersection individually, an optimization model is established with the effective green time of each phase and three schemes as decision variables. A right-turn vehicle and pedestrian conflict delay model is developed based on the pedestrian-vehicle interaction behavior as the constraints of the optimization model. The NSGA-II algorithm is used to solve the model, and the quantitative criteria for the exclusive right-turn lane and phase are obtained by sensitivity analysis. The results of this paper can be used as a guide for traffic design and for planning and controlling the operation of right-turning vehicles at intersections.

1. Introduction

Intersections have multiple traffic flows in different directions; the essence of signal control is to give each traffic flow the right of way in time to minimize conflicts and improve traffic safety. In the Chinese traffic scenario, right-turning vehicles are typically permitted to traverse intersections at any stage, potentially leading to interactions with pedestrian flow [1] within crosswalks. According to the latest road traffic safety law, these right-turning motor vehicles are obligated to reduce their speed when navigating crosswalks, with pedestrians holding an absolute right of way. Such traffic regulations are implemented indiscriminately at all intersections, resulting in a serious reduction in the capacity of the right-turn lane and even the intersection. However, without considering such phenomenon, the current right-turn resource allocation strategy cannot satisfy the traffic demand.

The spatiotemporal resource allocation schemes for right-turning vehicles at intersections include the setting of exclusive right-turn lanes and phases. Compared with shared lanes, exclusive right-turn lanes will eliminate delays to right-turning traffic at the red time [2], which is suitable for intersections with high volumes of right-turning traffic, but will also reduce the space available for straight-ahead traffic. From a system perspective, the flow of straight traffic will also impact the boundary conditions of the exclusive lane. Since the exclusive right-turn phase eliminates the conflict between vehicles and pedestrians, vehicle delays are always reduced at four-phase intersections without the exclusive right-turn phase, when the pedestrian right of way is strictly enforced. However, the situation would be different if pedestrian crossing efficiency is considered.

Many scholars have studied the allocation of spatial and temporal resources at single-point intersections in terms of efficiency [3–6], safety [7, 8], and environmental friendliness [3, 9–11]. The benefits (e.g., conflict severity, delays, emissions, etc.) before and after the implementation of the scheme are used as indicators to obtain the lane function setting and signal timing schemes. There are also some studies focusing on the robustness of the signal control system [12]. In terms of the study population, most studies focus only on motor vehicles and consider buses when traffic priority signals are available at intersections [9, 13]. Some studies indirectly consider the effect of pedestrians on intersection traffic operations by adding constraints [9, 14, 15] but do not include pedestrian traffic efficiency in the objective function. The vast majority of studies [16–18] assumed no delays for right-turning vehicles because they could pass through the intersection at any phase stage. However, this model assumption does not apply to urban intersections with a certain amount of pedestrian traffic.

Compared with right-turn movements, left-turn movements [19] tend to receive more attention in countries that drive on the right, and therefore relatively few research results have been conducted for right-turn space-time resource allocation, focusing more on the analysis of the yielding behavior of right-turning vehicles and pedestrians. Schmidt and Farber [20] point out that drivers mainly use parameters of body language, such as leg and head movements or body rotation to predict the intention of the pedestrian and thus decide whether to yield to the pedestrian. Muley et al. [21] investigated the factors influencing pedestrians crossing right-turning motor vehicle flows in the exclusive right-turn lane and showed that waiting behavior is independent of pedestrian characteristics and depends only on right-turning traffic characteristics. However, under the current road regulations in China, pedestrians have absolute priority in the right of way and right-turning vehicles should give way unconditionally.

Vehicle trajectory can well describe the vehicle motion information in various scenarios [22]. The two-dimensional movement of right-turning vehicles at intersections is a complex traffic issue. How to appropriately describe the driving trajectory of vehicles at intersections is a topic that many academics are dedicated to researching. Taking into account the interaction between various traffic flows, Ma et al. [23] established a two-dimensional simulation model based on a traditional social force model to characterize the turning behaviors of vehicles at crossings. Zhao et al. [24] developed a two-dimensional vehicle motion model for intersections under the presumption of optimal control, with the goal of minimizing terminal costs and operating costs. The dynamics of the vehicle motion are formulated in distance, which is different from traditional approaches. On this basis, Zhao et al. [25] considered the impact of vehicle interactions and added the safety cost of vehicle operation as the objective function to reconstruct the model. The new model can not only describe vehicle trajectories but also properly predict the sequence of vehicles passing through, making it possible to simulate intersection traffic flow more accurately.

Some scholars have also conducted studies on the signal control of right-turning motor vehicles. Wang et al. [26] studied the right-turn signal timing method under mixed traffic and verified that the conflicts between vehicles and bicycles were significantly reduced after setting right-turn signals. Wu et al. [27] proposed a signal control model based on the "Degree of Clustered Conflict" and formulated the right-turn lane signal control logic considering the conflict delay and potential accident risk.

However, previous studies of the spatiotemporal resource allocation scheme for right-turning vehicles only considered right-turning vehicle-related metrics, ignoring the impact on pedestrians and traffic flow in other directions at the intersection, and did not simultaneously optimize lane function and overall intersection signal timing to reduce pedestrian-vehicle delays. This study establishes a comprehensive framework to optimize the allocation of intersection time resources and right-turn space resources under different yielding ratios and volume levels by considering both vehicle and pedestrian efficiency in the context of new traffic regulations and proposes conditions for setting exclusive right-turn lanes and phases. The results can be applied to actual road scenarios and are of great significance to the improvement of right-turning traffic at intersections.

2. Spatiotemporal Resource Allocation Scheme for Right-Turning Vehicles

In this paper, the optimization algorithm aims to minimize the vehicle and pedestrian delays, respectively, which are utilized as the measurement of traffic efficiency. However, due to the incompatibility of these two delays, instead of a unique solution comprehensively, the current solutions typically make a trade-off of each delay correspondingly to achieve the relative optimality. To ensure sufficient green time for pedestrian phases, motor vehicle travel times are bound to be shortened, leading to increased delays. To properly address the above demand, a new model with a multiobjective framework is developed in this paper to select and optimize the allocation of spatiotemporal resources of right-turning vehicles.

The phase diagrams of the three assignment schemes of the four-phase intersection are presented in Table 1. Among them, scheme 1 is the shared-lane case, and scheme 2 represents the case with an exclusive right-turn lane. In Schemes 1 and 2, the vehicles in each direction are permitted to right-turn on red. Considering that pedestrians at a four-phase intersection are usually released to the straight-ahead traffic in the same direction simultaneously, it is proposed to integrate the exclusive right-turn phase into the left-turn-protected phase to maximize the traffic flow per unit time at the intersection while avoiding conflicts between pedestrians and right-turning vehicles.

3. A Multiobjective Optimization Model of Spatiotemporal Resource Allocation Scheme for Right-Turning Vehicles

3.1. Model Assumptions. The assumptions in this paper are as follows:

(1) Each arm of the intersection is a two-way six-lane road with an exclusive left-turn lane.

Table 1: Phase diagram under each scheme.

Scheme	Phase diagram	Pedestrian-vehicle conflict	Delays caused by straight-ahead vehicles
1	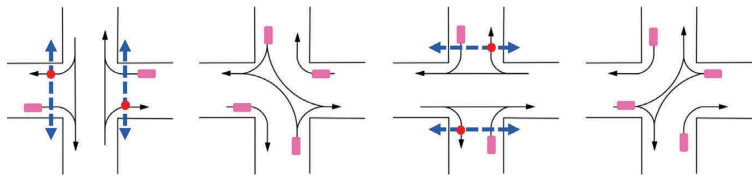	√	√
2	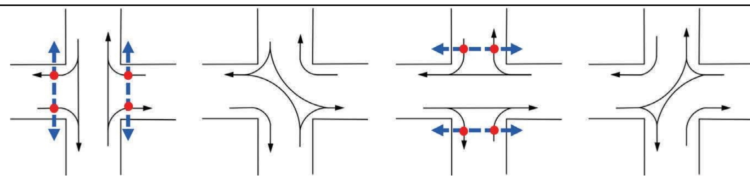	√	×
3	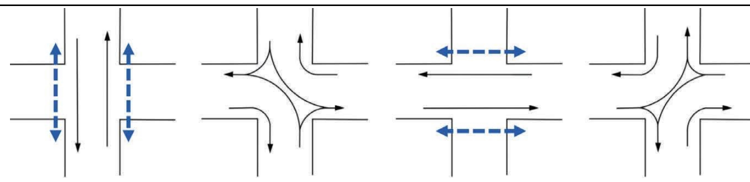	×	×

●Conflict points between pedestrians and right-turning vehicles. ▬Right-turning vehicles are blocked by queues of straight-through vehicles on red. ◀▶Pedestrian crossing flow lines.

(2) The intersection has unlimited vehicle queuing space, i.e., the short-lane scenario is not considered.

(3) As mutually independent events, pedestrians in both directions are assumed to cross without interfering with each other.

(4) Pedestrians can completely dissipate during the green time.

(5) Vehicles are assumed to merge into different lanes without merging delays.

(6) The traffic volumes arriving at each approach at the intersection are similar, so the right-turn resource allocation scheme used is consistent.

3.2. Notations. The layout of the intersections is shown in Figure 1. To facilitate subsequent illustration, the key symbols used are summarized in Table 2.

3.3. Optimization Model

3.3.1. Objective Function. The optimization objective is to maximize the traffic efficiency at the intersection for both motorists and pedestrians. For the given intersection, the first objective of the model mainly reflects the viewpoint of the vehicle driver, i.e., minimizing the average delay of all vehicles at the intersection under each scheme.

$$\min\,(1-\delta_1-\delta_2)D_1^v+\delta_1D_2^v+\delta_2D_3^v. \tag{1}$$

The second objective function reflects the pedestrian's perspective and aims to minimize the pedestrian crossing delay under each scheme.

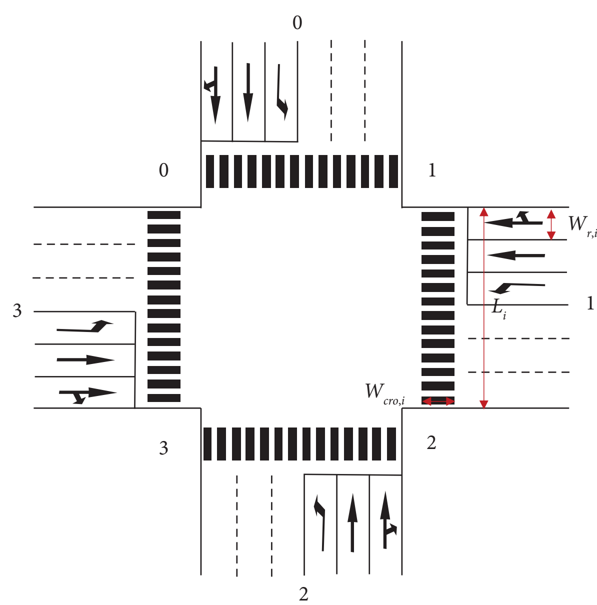

Figure 1: Intersection layout.

$$\min\,(1-\delta_1-\delta_2)D_1^p+\delta_1D_2^p+\delta_2D_3^p. \tag{2}$$

3.3.2. Decision Variables. The decision variables of the model include the right-turn lane type (δ_1), the right-turn phase type (δ_2), and the effective green time (g_u) of each phase.

3.3.3. Constraints. The following are common inequality constraints that limit the decision variables. Equations (3) and (4) restrict the cycle length and the green time of each

Table 2: Notations and parameters.

Notations	Meaning	Unit
i, j	Index of intersection arms (approaches) or corners, as shown in Figure 1, $i = 0, 1, 2, 3$	—
L_i	The length of the crosswalk at arm i	m
δ_1	The binary variable represents whether scheme 2 has been adopted, $\delta_1 = \begin{cases} 1, & \text{Scheme 2 has been adopted.} \\ 0, & \text{Scheme 2 hasn't been adopted.} \end{cases}$	—
δ_2	The binary variable represents whether scheme 3 has been adopted, $\delta_2 = \begin{cases} 1, & \text{Scheme 3 has been adopted.} \\ 0, & \text{Scheme 3 hasn't been adopted.} \end{cases}$	—
g_i^p	The effective green time of pedestrian signals at the approach i	s
g_u	The green time corresponding to the phase u of the phase sequence is shown in Table 1	
C	The cycle length	s
$C_{\min}, C_{\max}$	The minimum and the maximum length of cycle time	s
$g^u_{\min}, g^u_{,\max}$	The minimum and the maximum length of showing the green time of vehicular signal under the phase u	s
T_{red}	All-red interval	s
T_{yellow}	The duration of yellow light	s
P_{vtp}	The probability of a right-turn vehicle yielding to pedestrians	—
I_i^p	The pedestrian clearance time at the crosswalk of the arm i	s
v^p	The average speed of pedestrians crossing	m/s
v^{rtv}	The average speed of right-turn vehicles through intersections	km/h
$W_{r,i}$	The width of the right-turn lane at the arm i	m
$W_{\text{cro},i}$	The width of the crosswalk at the approach i	m
$d_i^{v,\text{sig}}$	The vehicular signal delay at the approach i	s
$d_{\text{ij}}^{p,\text{sig}}$	The pedestrian signal delay from the corner i to corner j	s
$d_i^{v,\text{con}}$	The vehicular conflict delay at the approach i	s
$d_{\text{ij}}^{p,\text{con}}$	The pedestrian conflict delay from the corner i to corner j	s
D_k^v	Average vehicle delay for all directions at intersections under the scheme k	s
D_k^p	Average pedestrian delay for all crosswalks at intersections under the scenario k	s

phase to a certain range. Equation (5) guarantees that there is and only one scheme is selected.

$$C_{\min} \leq C \leq C_{\max}, \tag{3}$$

$$g^u_{\min} \leq g_u \leq g^u_{\max}, \quad u = 1, 2, 3, 4, \tag{4}$$

$$0 \leq \delta_1 + \delta_2 \leq 1. \tag{5}$$

The model also includes the following equation constraints.

(1) The length of cycle time: The cycle length is the sum of the green, yellow, and all-red time for each phase, i.e.,

$$C = \sum_{u=1}^{4} \left(g_u + T_{\text{yellow}} + T_{\text{red}} \right). \tag{6}$$

(2) Pedestrian clearance time: The pedestrian clearance time is defined to ensure pedestrians have enough time to cross safely. It is determined based on the length of the crosswalk, pedestrian walking speed, and additional safety time.

$$I_i^p = \frac{L_i}{v^p} + t_s, \quad i = 0, 1, 2, 3. \tag{7}$$

(3) The green time: The green light durations of parallel crosswalks should be equal. The sum of the pedestrian green light and flashing light duration should be no greater than the vehicle display green light duration, which is considered here as a binding constraint, taking the case where the equal sign holds.

$$\begin{gathered} g_i^p = g_{i+2}^p, \quad i = 0, 1, \\ g_0^p + \max\left(I_0^p, I_2^p\right) = g_1, \\ g_1^p + \max\left(I_1^p, I_3^p\right) = g_3. \end{gathered} \tag{8}$$

In addition, the delay model expressions (equations (11)–(15)) developed collectively constitute the constraints of this model.

4. Vehicle and Pedestrian Delay Models

In this optimization problem, the delays mainly originate from

(1) Signal control: Traffic objects at the intersection can only pass during the green time (except for right-turning vehicles under Scheme 1 or Scheme 2), which can cause signal delay. In addition, the

blocking delays of right-turning vehicles under Scheme 1 are also included in the signal control delays, which are caused by straight-ahead vehicles occupying the shared lane queue during the red time.

(2) Conflict delay: Delay caused by right-turning vehicles without signal control passing through the conflict area together with pedestrians. Conflict delays exist for both right-turning motor vehicles and pedestrians for Schemes 1 and 2.

4.1. Signal Delay Model. The average delay for both vehicles and pedestrians under signal control is calculated according to the control delay model in HCM2010 [28]. Where vehicle delays are calculated by lane group, the blocking delays of straight-ahead vehicles to right-turning vehicles will be included in this signal delay, as in the following equation:

$$d_i^{v,\mathrm{sig}} = d_{1i}(\mathrm{PF}) + d_{2i} + d_{3i}. \tag{9}$$

The average signal delay for pedestrians [28] is calculated according to the following equation:

$$d_i^{p,\mathrm{sig}} = \frac{\left(C - g_i^p\right)^2}{2C}. \tag{10}$$

4.2. Conflict Delay Model. The calculation of conflict delay is based on the gap theory. For right-turning vehicles and pedestrians at a four-phase signal intersection, conflicts are generated only when the pedestrian signal is green. Two scenarios (concentrated pedestrian arrival and random pedestrian arrival) can be classified, as shown in Figure 2.

During the pedestrian red time, right-turning vehicles are allowed to cross the intersection without restriction, while pedestrians have to wait. Therefore, at the beginning of the pedestrian green time, there is a concentration of pedestrians arriving at the conflict zone. At this point, the right-turning vehicles need to wait for these pedestrians to pass through the conflict zone until they can find a chance to cross the intersection. When the concentration of pedestrians arrives, it is assumed that they are arranged in a matrix through the conflict zone, so the right-turn vehicle delay can be calculated by the following equation:

$$d_i^{v,\mathrm{con1}} = \frac{L_{\mathrm{ped}} + W_{r,i}}{v_P} = \frac{\left(\lambda_{\mathrm{P}} T_{\mathrm{Pred}} k_P / 3600 W_{cro,i}\right) + W_{r,i}}{v_P}, \tag{11}$$

where L_{ped} is the length of the pedestrian matrix, T_{Pred} is the pedestrian red time, and k_P is the average area occupied by pedestrians.

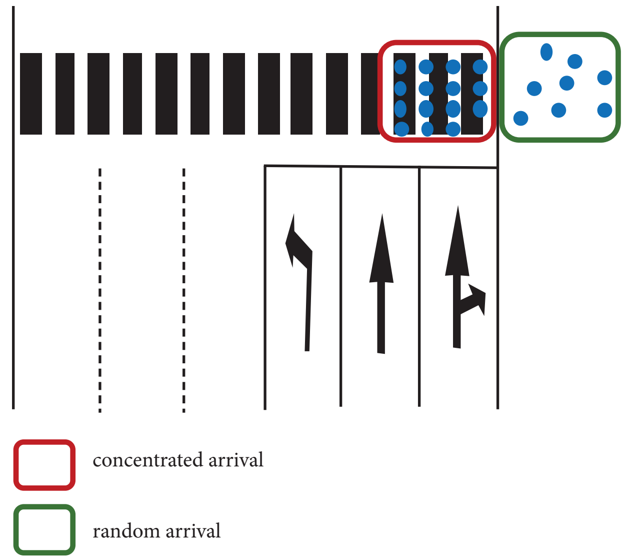

Figure 2: Pedestrian arrival form.

When pedestrians arrive randomly, considering the arrival intensity of pedestrians in both directions, the delay [29] of right-turning vehicles can be calculated by the following equations:

$$d_i^{v,\mathrm{con2}} = P_{\mathrm{vtp}} \frac{\lambda T_{P\,\mathrm{green}} + \exp\left(-\lambda \cdot T_{P\,\mathrm{green}}\right) - 1}{\lambda^2 T_{P\,\mathrm{green}}}, \tag{12}$$

$$\lambda = \frac{\left(\lambda_i^{\mathrm{mn}} + \lambda_i^{\mathrm{nm}}\right) \exp\left(-\left(\lambda_i^{\mathrm{mn}} + \lambda_i^{\mathrm{nm}}\right) G_{\mathrm{safe}} / 3600\right)}{3600}, \tag{13}$$

where $T_{P\mathrm{green}}$ is the pedestrian green time, λ_i^{mn} is the pedestrian arrival intensity from corner m to corner n at approach i, and G_{safe} is the safe traversable clearance, which can be calculated by the following equation:

$$G_{\mathrm{safe}} = \frac{W_r}{v^P} + \frac{W_{\mathrm{cro}}}{v^{\mathrm{rtv}}} * 3.6 + t_s, \tag{14}$$

where t_s is the time taken by a right-turning vehicle to pass the conflict zone.

The conflict delay for pedestrians [30] in this scenario is

$$d_i^{p,\mathrm{con}} = \left(1 - P_{\mathrm{vtp}}\right) \frac{e^{\mu_i G_{\mathrm{safe}}} - \mu_i G_{\mathrm{safe}} - 1}{\mu_i}, \tag{15}$$

where μ_i is the arrival intensity of right-turning vehicles, including right-turning traffic in both directions (arriving and exiting approach i). In scheme 1 (i.e., the shared lane case), the right-turning vehicles exiting approach i are blocked by the straight-ahead traffic and cannot pass the intersection during the red time, so there is right-turning traffic in only one direction.

In summary, all delays have been modeled. Since the vehicle and pedestrian delays vary under different scenarios and in different directions, it is also necessary to obtain the average delay by weighting the respective flows.

5. Solution Algorithm and Sensitivity Analysis

For the multiobjective optimization problem (MOP) in this study, there is no absolute optimal solution but only a set of "noninferior solutions." The "noninferior solution" in this study refers to the fact that among the combinations of spatiotemporal resource allocation scheme and signal duration allocation, the selected combination reduces at least one of the pedestrian delay or motor vehicle delay when it is not possible to reduce both. The values of such a set of decision variables are taken as a noninferior solution, i.e., a Pareto optimal solution. In this paper, all noninferior solutions are generated by the optimization algorithm and are selected based on the research problem.

5.1. Algorithm Comparison and Modeling Results. From the model structure, the problem in this study is a nonlinearly constrained optimization problem. Due to the complexity and multiplicity of objective functions and constraints, traditional optimization algorithms have difficulty in finding the global optimal solution of this problem smoothly and quickly.

In this study, a heuristic algorithm is employed to tackle the MOP. Various multiobjective evaluation algorithms are available, broadly categorized into three categories: domination-based framework, indicator-based framework, and decomposition-based framework [31]. Given the unknown Pareto frontier of the proposed MOP, it is amenable to resolution by either the first or third type of evolutionary algorithm.

One of the most renowned multiobjective optimization algorithms is the nondominated sorting genetic algorithm II (NSGA-II), introduced by Deb's team in 2001 [32]. This algorithm optimizes MOPs by simultaneously optimizing all objectives.

Drawing inspiration from decomposition-based concepts, the reference vector guided evolutionary algorithm (RVEA) was proposed [33] to achieve better approximation of frontier surfaces in high-dimensional spaces. RVEA leverages a scalarization approach, known as angle-penalized distance, to balance solution convergence and diversity within high-dimensional objective spaces.

To solve the model in this paper, the Python solver Pymoo [34] is employed. The termination condition of the algorithm is set as follows: the average variance in the target space is below 0.25% and the difference with the constraints is within 10^{-6}; meanwhile, the maximum number of iterations is set to 1000.

Regarding the primary algorithm parameters, they are configured as follows:

(1) Population Size (PS): To strike a balance between global search capability and computational complexity, two population sizes of 200 and 400 were selected for solving the model, considering its relative complexity. A larger population size enhances global search potential, reducing the risk of local optima.

Table 3: Parameters and their values.

Parameter	Value
$C_{\min}$	60
$g^{u}_{\min}$	Max (10, I^{p}_{u})
v^{p}	1.2
$W_{r,i}$	3.5
T_{red}	1
t_s	1
$C_{\max}$	120
$g^{u}_{,\max}$	50
v^{rtv}	15
$W_{\text{cro},i}$	4
T_{yellow}	3

(2) Crossover Probability (CP): The crossover operation plays a pivotal role in generating new individuals within evolutionary algorithms. Crossover probability significantly influences search efficiency and convergence speed. A value that is too large may introduce excessive randomness into the search process, affecting algorithm performance, while a value that is too small can limit the search range and impede convergence. Hence, two scenarios with crossover probabilities of 0.6 and 0.9 are examined.

(3) Mutation Probability (MP): The mutation operation is an auxiliary mechanism for generating new individuals, dictating the local search capacity of the evolutionary algorithm. Generally falling within the range of 0.01 to 0.1, this study prioritizes strong search capability and assesses mutation probabilities of 0.05 and 0.1.

The optimal solution of the model is determined according to the multicriteria decision making criterion , i.e., by introducing an augmented scalarization function that assigns certain weights to the two objectives. In this paper, both vehicles and pedestrians are considered two types of traffic bodies, and the weights of the respective objectives are determined by the total traffic flow of each traffic body.

Meanwhile, based on the actual road traffic situation in China, the internal parameters of the optimization model are set as shown in Table 3. The parameter values linked to intersection geometric design are acquired from actual survey data, while the parameter values related to signal timing are taken from a reference [16].

Assume that all vehicles and pedestrians have no violations; that is, the probability of yielding to right-turning vehicles is taken as 1. The optimization model is solved for a one-way pedestrian arrival rate of 500 pedestrian/hour (ped/h) with 300 vehicles/hour (veh/h) of left-turning traffic, 300 veh/h of straight-through traffic, and 50 veh/h of right-turning traffic, respectively.

To comprehensively evaluate the algorithms' robustness and effectiveness across diverse parameter configurations, we conducted 500 runs using different random seeds to solve the model. These runs incorporated different parameter and algorithm settings, and the results of the 500 iterations, encompassing the average execution time (AET), the average delay of vehicles (ADV), the average delay of pedestrians

Table 4: Comparison of algorithms for different parameter values.

Algorithm	PS	CP	MP	AET	ADV	ADP	VDV	VDP
NSGA-II	400	0.9	0.05	**18.146**	**72.160**	**37.306**	0.088	**0.007**
	400	0.9	0.1	**16.049**	**72.155**	37.315	0.098	0.008
	400	0.6	0.05	19.157	72.200	37.309	0.124	0.015
	400	0.6	0.1	**18.113**	72.223	37.307	0.155	0.018
	200	0.9	0.05	24.687	72.213	37.312	0.177	0.020
	200	0.9	0.1	24.576	**72.195**	37.312	0.169	0.021
	200	0.6	0.05	27.076	72.239	**37.307**	0.232	0.027
	200	0.6	0.1	26.222	72.455	**37.283**	0.309	0.034
RVEA	400	0.9	0.05	39.613	72.213	37.310	**0.079**	**0.008**
	400	0.9	0.1	39.733	72.209	37.310	0.089	**0.008**
	400	0.6	0.05	47.900	72.212	37.309	**0.045**	0.008
	400	0.6	0.1	47.470	72.205	37.309	0.090	0.009
	200	0.9	0.05	26.842	72.239	37.307	0.084	0.009
	200	0.9	0.1	26.710	72.196	37.311	0.094	0.008
	200	0.6	0.05	32.308	72.230	37.309	**0.074**	0.010
	200	0.6	0.1	31.824	72.244	37.307	0.077	0.009

The bold values in the table are the smallest top three values in each column, allowing for a more intuitive comparison of the performance of the algorithms under different parameter choices.

(ADP), the variance of vehicle delay (VDV), and the variance of pedestrian delay (VDP) [35], are presented in Table 4.

Table 4 reveals that the model's overall performance is optimized when employing the first set of parameters with the NSGA-II. Under these optimal parameter settings, we successfully obtained a set of dominant and optimal solutions using NSGA-II, as shown in Figure 3.

According to the optimal solution, scheme 1 is selected with an effective green time of 14.33 s, 12.93 s, 14.33 s, and 13.03 s for each phase, corresponding to the vehicle delay of 72.11 s and the pedestrian delay of 37.31 s for the objective function.

The focus of this study is to obtain the setting conditions for the exclusive right-turn lane and phase for a single approach, so as to simplify the structure of the optimization model and improve the computational accuracy. The paper assumes a balanced arrival flow for each approach at the intersection. In addition, the multiobjective optimization framework proposed in this study is well-scalable and can be adapted to actual road scenarios.

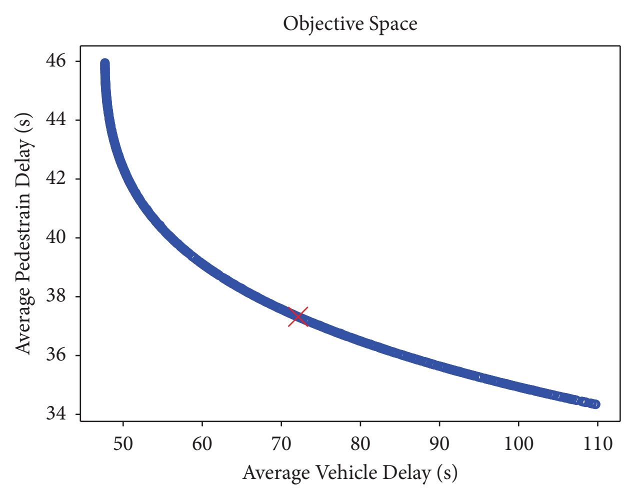

Figure 3: Model result.

5.2. Sensitivity Analysis. To obtain the boundary conditions for the exclusive right-turn lane and phase settings, the traffic demand in each direction on all approaches is assumed to be equal, and the optimal solution is obtained by the previously proposed multiobjective optimization framework. In this paper, we focus on four parameters, namely, vehicle yield probability, straight-ahead vehicle volume, right-turn motor vehicle volume, and pedestrian volume. Assuming that the arrival rate of left-turning vehicles is always 300 veh/h, the following results are obtained.

5.2.1. Vehicle Delay. In Figure 4, the x, y, and z coordinates denote the arrival rate of right-turning vehicles, the arrival rate of straight-ahead vehicles, and the vehicle delay, respectively. Under the different combinations of the yielding probability and one-way pedestrian arrival intensity, the vehicle delays of the optimal spatiotemporal allocation schemes show the same distribution pattern.

Overall, the average motor vehicle delay increases with the increasing arrival rate of right-turning and straight-ahead vehicles and pedestrians, as well as the probability of yielding. In the case of a low arrival rate of straight-ahead traffic, the delay decreases as the arrival rate of right-turning vehicles increases. This is because delays in the low-volume scenario are primarily generated by signal control while right-turning vehicles are not. The more right-turning vehicles arrive, the lower the average delay for all vehicles.

5.2.2. Pedestrian Delay. Assume that the arrival rates of straight-ahead traffic are 100 vehicles/h (veh/h) and 300 veh/h, and the one-way arrival rates of pedestrians are 50 pedestrians/h (ped/h), 250 ped/h, and 450 ped/h. Figure 5 shows the variation of the average pedestrian delay with

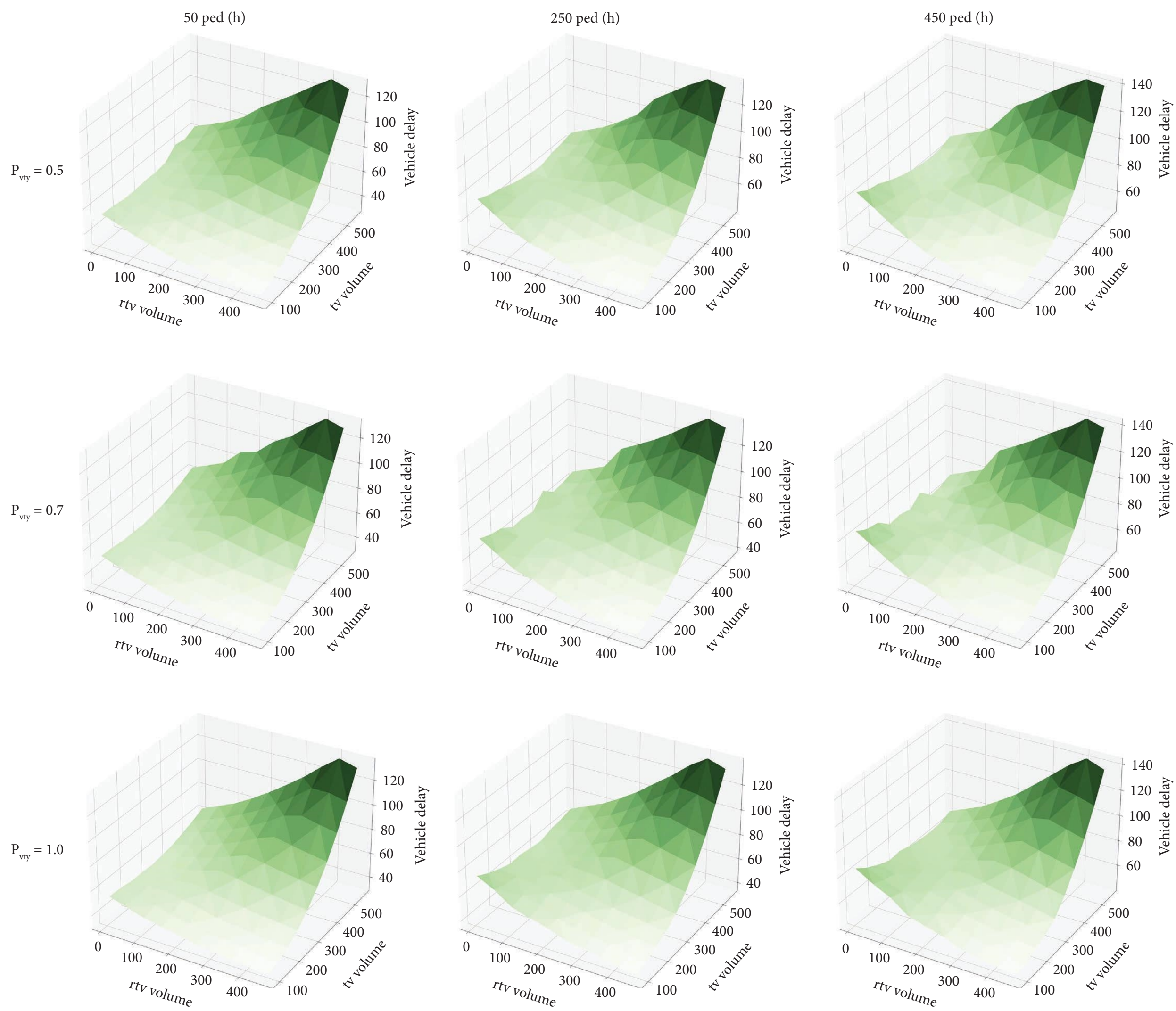

Figure 4: Average vehicle delay.

respect to the right-turning motor vehicle flow for the optimal scheme with different vehicle yield probabilities.

In this paper, multiobjective optimization is performed with the total number of pedestrians and vehicles as their respective weights, so there may be situations when delays at low pedestrian flows will be higher than delays at high pedestrian flows.

Pedestrian delay is relatively low and changes more gently as the probability of vehicles yielding to pedestrians increases. At lower straight-ahead traffic volumes, the average pedestrian delay increases with higher right-turning arrival rates, which is generally caused by the increased conflict delays between pedestrians and right-turning vehicles. At higher straight-ahead volumes, the change in average pedestrian delay decreases and then increases. This is because, with the increase in right-turn traffic flow, the allocation of the intersection spatiotemporal resource scheme is adjusted, resulting in a decrease in signal delay greater than the increase in conflicting delay, which ultimately leads to a decreasing trend in the average pedestrian delay. Especially, when $P_{\mathrm{vtp}} = 1$, the delay of pedestrians is entirely due to signal control. Shared lanes are typically employed when there is low right-turn traffic volume. In this lane situation, the signal timing scheme at the intersection is affected by the volume of right-turning vehicles, resulting in changes in pedestrian delay. When the flow of right-turn vehicles reaches the critical threshold for setting an exclusive right-turn lane, the intersection signal timing scheme is no longer impacted. At this time, the delay of pedestrians essentially remains stable, as shown in the last subgraph of Figure 5.

5.2.3. Spatiotemporal Resource Allocation Scheme. Figure 6 (horizontal coordinates are the arrival rates of straight-ahead traffic and vertical coordinates are the arrival rates of right-turning vehicles) gives the optimal schemes for different vehicles yielding probabilities at one-way pedestrian arrival intensities of 50 ped/h, 250 ped/h, and 450 ped/h. In Figure 6, the horizontal coordinates denote the arrival rate of straight-ahead traffic, and the vertical coordinates denote the arrival rates

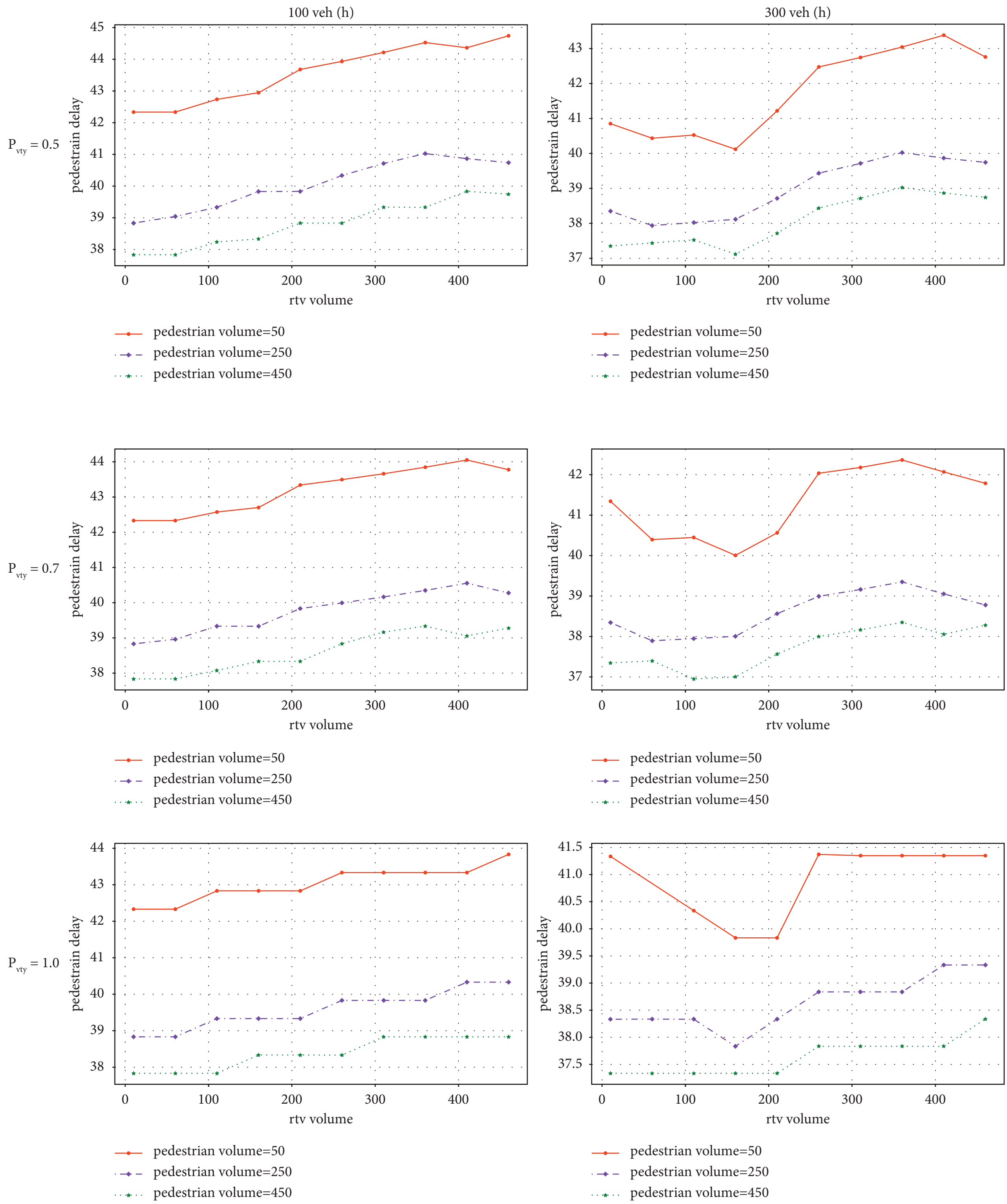

Figure 5: Average pedestrian delay.

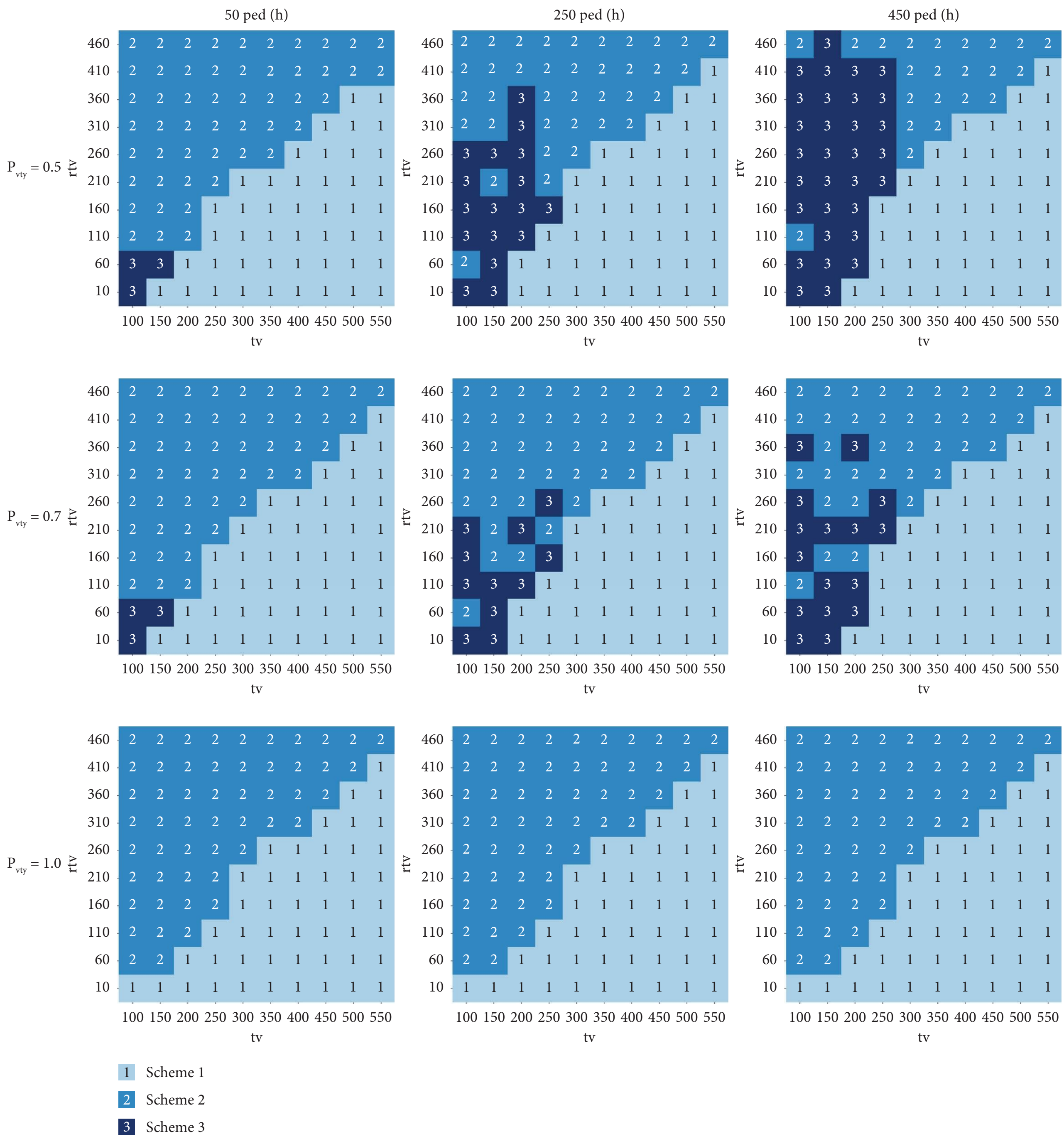

Figure 6: Optimal spatiotemporal resource allocation scheme.

of right-turning vehicles. From Figure 6, the conditions of exclusive right-turn lane and phase can be summarized as follows:

(1) Exclusive right-turn lane: As shown in Figure 6, the setting of the exclusive right-turn lane is mainly influenced by the flow of straight-ahead traffic and

the flow of right-turning traffic. When the arrival rate of right-turning vehicles reaches 310 veh/h and does not exceed the arrival rate of straight-ahead traffic, or the ratio of right-turning vehicles to the arrival flow of straight-ahead traffic reaches 0.7, it is appropriate to set up an exclusive right-turn lane.

(2) Exclusive right-turn phase: The setting of the exclusive right-turn phase is also affected by the pedestrian flow and vehicle yielding probability. Theoretically, the intersections with strict enforcement of pedestrian right of way do not require an exclusive right-turn phase, which is consistent with the results of the model.

In the case where vehicles and pedestrians have equal right of way ($P_{vtp} < 1$), the optimal solution is derived considering both pedestrian and vehicle delays, resulting in a decision result that does not present a clear quantitative pattern. Therefore, it is difficult to obtain the setting conditions for the exclusive right-turn phase directly from the model results.

Comparing the distributions under different pedestrian volume levels, it can be considered appropriate to set an exclusive right-turn phase when the vehicle yielding rate is lower than 0.7 and the one-way pedestrian arrival rate reaches 450 ped/h based on the setting of an exclusive right-turn lane.

6. Conclusion

In this paper, three right-turn space-time resource allocation schemes are proposed. A multiobjective optimization framework for the four-phase intersection considering both vehicular and pedestrian traffic efficiency is developed, and the delay model considering pedestrian-vehicle interaction behavior and pedestrian crossing form is established. Based on this framework, the optimal right-turn space-time resource allocation scheme and intersection signal timing scheme can be derived for different pedestrian and vehicular traffic levels and vehicle yielding probabilities. From the results of the optimization model, it is appropriate to set an exclusive right-turn lane when the arrival rate of right-turn vehicles reaches 310 veh/h and is not higher than the arrival rate of straight-ahead vehicles or the ratio of right-turn vehicles to the arrival flow of straight-ahead vehicles reaches 0.7. The setting conditions for the exclusive right-turn phase are that the yielding rate of vehicles is less than 0.7 and the arrival rate of one-way pedestrians reaches 450 ped/h based on the exclusive right-turn lane setting conditions.

The optimization model developed in this paper has good scalability and can be adjusted to better predict vehicle and pedestrian delays according to the actual road conditions. In addition, besides traffic efficiency, nonmotorized traffic is also an important factor affecting the right-turn space and time resource allocation at intersections. This needs to be studied in depth in the future to further clarify the conditions for setting exclusive right-turn lanes and phases.

Data Availability

The data used to support the findings of this study are included within the paper.

Conflicts of Interest

The authors declare that they have no conflicts of interest regarding the publication of this paper.

Acknowledgments

This work was financially supported by the National Natural Fund Project (Grant no. 52272320).

References

[1] X. Chen, C. Shao, and Y. Hao, "Influence of pedestrian traffic on capacity of right-turning movements at signalized intersections," *Transportation Research Record*, vol. 2073, no. 1, pp. 114–124, 2008.

[2] P. Chen, H. Qi, and J. Sun, "Investigation of saturation flow on shared right-turn lane at signalized intersections," *Transportation Research Record*, vol. 2461, no. 1, pp. 66–75, 2014.

[3] H. Jia, Y. Lin, Q. Luo, Y. Li, and H. Miao, "Multi-objective optimization of urban road intersection signal timing based on particle swarm optimization algorithm," *Advances in Mechanical Engineering*, vol. 11, no. 4, Article ID 168781401984249, 2019.

[4] A. Jamal, M. Tauhidur Rahman, H. M. Al-Ahmadi, I. Ullah, and M. Zahid, "Intelligent intersection control for delay optimization: using meta-heuristic search algorithms," *Sustainability*, vol. 12, no. 5, p. 1896, 2020.

[5] X. Song, Y. Zhang, and M. Lin, "An optimization model for dynamic lane grouping and signal phase at intersection," *Journal of Transporation Systems Engineering & Information Technology*, vol. 20, no. 6, pp. 121–128, 2020.

[6] C. Zhai, F. Luo, Y. Liu, and J. Xu, "Adaptive control of isolated intersections based on sequential signal-stage optimisation," *Proceedings of the Institution of Civil Engineers – Transport*, vol. 174, no. 3, pp. 170–181, 2021.

[7] F. Wang, K. Tang, K. Li, Z. Liu, and L. Zhu, "A group-based signal timing optimization model considering safety for signalized intersections with mixed traffic flows," *Journal of Advanced Transportation*, vol. 2019, Article ID 2747569, 13 pages, 2019.

[8] Y. Su, D. Yao, Y. Zhang, Z. Li, L. Li, and W. Zheng, "Vehicle/Pedestrian conflict analysis and exclusive right-turn phase setting study," *Proceedings of IEEE Intelligent Vehicle Symposium*, pp. 733–738, 2008.

[9] E. Christofa, I. Papamichail, and A. Skabardonis, "Person-based traffic responsive signal control optimization," *IEEE Transactions on Intelligent Transportation Systems*, vol. 14, no. 3, pp. 1278–1289, Sept. 2013.

[10] W. Kou, X. Chen, L. Yu, and H. Gong, "Multiobjective optimization model of intersection signal timing considering emissions based on field data: a case study of Beijing," *Journal of the Air & Waste Management Association*, vol. 68, no. 8, pp. 836–848, 2018.

[11] Q. H. Tran, V. M. Do, and T. H. Dinh, "Traffic signal timing optimization for isolated urban intersections considering environmental problems and non-motorized vehicles by using constrained optimization solutions," *Innovative Infrastructure Solutions*, vol. 7, no. 5, p. 299, 2022.
[12] Y. Han, Z. Xu, and H. Guo, "Robust predictive control of a supercavitating vehicle based on time-delay characteristics and parameter uncertainty," *Ocean Engineering*, vol. 237, Article ID 109627, 2021.
[13] X. Li and D. Li, "Dynamic self-adaptive chaotic particle swarm optimization algorithm in optimal control of public transit priority traffic signal," in *Proceedings of the 10th International Conference Intelligence Human-Machine Systems and Cybernetics, IHMSC 2018*, August 2018.
[14] C. K. Wong and S. C. Wong, "Lane-based optimization of signal timings for isolated junctions," *Transportation Research Part B: Methodological*, vol. 37, no. 1, pp. 63–84, 2003.
[15] Z. Yang, J. Ma, B. Wang, and L. Gen, "Intersection signal timing optimization model considering pedestrian protection strategies," *Journal of Transporation Systems Engineering & Information Technology*, vol. 21, no. 3, pp. 71–77, 2021.
[16] W. Ma, Y. Liu, and K. L. Head, "Optimization of pedestrian phase patterns at signalized intersections: a multi-objective approach," *Journal of Advanced Transportation*, vol. 48, no. 8, pp. 1138–1152, 2014.
[17] W. Ma, D. Liao, Y. Liu, and H. K. Lo, "Optimization of pedestrian phase patterns and signal timings for isolated intersection," *Transportation Research Part C: Emerging Technologies*, vol. 58, pp. 502–514, 2015.
[18] C. Yu, W. Ma, K. Han, and X. Yang, "Optimization of vehicle and pedestrian signals at isolated intersections," *Transportation Research Part B: Methodological*, vol. 98, pp. 135–153, 2017.
[19] L. Chen, C. Chen, and R. Ewing, "Left-turn phase: permissive, protected, or both? A quasi-experimental design in NewYork City Acc," *Accident Analysis & Prevention*, vol. 76, pp. 102–109, 2015.
[20] S. Schmidt and B. Farber, "Pedestrians at the kerb-Recognising the action intentions of humans," *Transportation Research Part F: Traffic Psychology and Behaviour*, vol. 12, no. 4, pp. 300–310, 2009.
[21] D. Muley, M. Kharbeche, W. Alhajyaseen, and M. Al-Salem, "Pedestrians' crossing behavior at marked crosswalks on channelized right-turn lanes at intersections," *Procedia Computer Science*, vol. 109, pp. 233–240, 2017.
[22] X. Chen, Z. Wang, Q. Hua, W. L. Shang, Q. Luo, and K. Yu, "AI-empowered speed extraction via port-like videos for vehicular trajectory analysis," *IEEE Transactions on Intelligent Transportation Systems*, vol. 24, no. 4, pp. 4541–4552, 2023.
[23] Z. Ma, J. Xie, X. Qi, Y. Xu, and J. Sun, "Two-dimensional simulation of turning behavior in potential conflict area of mixed-flow intersections," *Computer-Aided Civil and Infrastructure Engineering*, vol. 32, no. 5, pp. 412–428, 2017.
[24] J. Zhao, V. L. Knoop, and M. Wang, "Two-dimensional vehicular movement modelling at intersections based on optimal control," *Transportation Research Part B: Methodological*, vol. 138, pp. 1–22, 2020.
[25] J. Zhao, V. L. Knoop, and M. Wang, "Microscopic traffic modeling inside intersections: interactions between drivers," *Transportation Science*, vol. 57, no. 1, pp. 135–155, 2023.
[26] D. Wang, C. Liang, and T. Feng, "Signal timing method of right-turn vehicles based on mixed traffic," *Journal of Harbin Institute of Technology*, vol. 41, no. 10, pp. 251–254, 2009.
[27] Z. Wu, L. Zhao, and J. Sun, "A study of dynamic right-turn signal control strategy at mixed traffic flow intersections," *Prometheus*, vol. 26, no. 6, pp. 449–458, 2014.
[28] Transportation Research Board Highway, *Capacity Manual*, Transportation Research Board: National Research Council, Washington, DC, USA, 2010.
[29] B. Li, Z. Wang, M. Ma, H. Yang, and F. Yue, "Capacity and delay of right-turn vehicles at signalized intersections under influence of pedestrian two-stage crossing," *Journal of Transporation Systems Engineering & Information Technology*, vol. 22, no. 2, pp. 257–267, 2022.
[30] K. M. Chen, X. Q. Luo, H. Ji, and Y. D. Zhao, "Towards the pedestrian delay estimation at intersections under vehicular platoon caused conflicts," *Scientific Research and Essays*, vol. 5, no. 9, pp. 941–947, 2010.
[31] A. Trivedi, D. Srinivasan, K. Sanyal, and A. Ghosh, "A survey of multiobjective evolutionary algorithms based on decomposition," *IEEE Transactions on Evolutionary Computation*, vol. 21, no. 3, pp. 1–462, 2016.
[32] K. Deb, A. Pratap, S. Agarwal, and T. Meyarivan, "A fast and elitist multiobjective genetic algorithm: nsga-II," *IEEE Transactions on Evolutionary Computation*, vol. 6, no. 2, pp. 182–197, 2002.
[33] R. Cheng, Y. Jin, M. Olhofer, and B. Sendhoff, "A reference vector guided evolutionary algorithm for many-objective optimization," *IEEE Transactions on Evolutionary Computation*, vol. 20, no. 5, pp. 773–791, 2016.
[34] J. Blank and K. Deb, "Pymoo: multi-objective optimization in Python," *IEEE Access*, vol. 8, pp. 89497–89509, 2020.
[35] S. Verma, M. Pant, and V. Snasel, "A comprehensive review on NSGA-II for multi-objective combinatorial optimization problems," *IEEE Access*, vol. 9, pp. 57757–57791, 2021.